Sponsored by

DEFENSE ADVANCED RESEARCH PROJECTS AGENCY

Accesion For	
NTIS CRA&I	X
DTIC TAB	☐
Unannounced	☐
Justification per AD A253125	
By	
Distribution /	
Availability Codes	
Dist	Avail and / or Special
A-1	

OPTOELECTRONICS MATERIAL CENTER

A Collaborative Program including

Center for High Technology Materials of the University of New Mexico

Stanford University

California Institute of Technology

ARPA Order No. 7526
Issued by DARPA/CMO under contract #MDA972-90-C-0046

REPORT DOCUMENTATION PAGE	Form Approved OMB No. 0704-0188

1. AGENCY USE ONLY *(Leave blank)*

2. REPORT DATE
October 19, 1992

3. REPORT TYPE AND DATES COVERED
Quarterly 1 Jan. 92 to 31 March 92

4. TITLE AND SUBTITLE
Optoelectronic Materials Center, A Collaborative Program Including University of New Mexico, Stanford University and California Institute of Technology

5. FUNDING NUMBERS
MDA972-90-C-0046

6. AUTHOR(S)
S.R.J. Brueck, Editor

7. PERFORMING ORGANIZATION NAME(S) AND ADDRESS(ES)
University of New Mexico
Center for High Technology Materials
EECE Building, Room 125
Albuquerque, NM 87131

8. PERFORMING ORGANIZATION REPORT NUMBER
Qtr

9. SPONSORING/MONITORING AGENCY NAME(S) AND ADDRESS(ES)
Defense Advanced Research Projects Agency
ARPA Order No. 7526 Issued by DARPA/CMO
under contract #MDA972-90-C-0046

92-28029

411243

12P8

11. SUPPLEMENTARY NOTES

12a. DISTRIBUTION/AVAILABILITY STATEMENT

12b. DISTRIBUTION CODE

13. ABSTRACT *(Maximum 200 words)*

The Optoelectronic Materials Center is a collaborative program involving the University of New Mexico, Stanford University, and the California Institute of Technology. Sandia National Laboratories and MIT Lincoln Laboratory are also involved in this program under separate contract vehicles. This program emphasizes three main areas:

- diode-based visible sources
- two-dimensional optical interconnects, and
- high-speed optoelectronics.

Progress on individual tasks is very briefly discussed below. Several of the tasks will impact more than one of the above areas. For simplicity, the tasks are arranged by institution in an order roughly determined by the above areas.

14. SUBJECT TERMS
Diode based visible sources, two dimensional optical interconnects, High speed Optoelectronics.

15. NUMBER OF PAGES
11 plus cover

16. PRICE CODE

17. SECURITY CLASSIFICATION OF REPORT	18. SECURITY CLASSIFICATION OF THIS PAGE	19. SECURITY CLASSIFICATION OF ABSTRACT	20. LIMITATION OF ABSTRACT
	Unclassified	Unclassified	

NSN 7540-01-280-5500

Standard Form 298 (Rev. 2-89)
Prescribed by ANSI Std Z39-18
298-102

DARPA OPTOELECTRONICS CENTER

QUARTERLY REPORT

January 1, 1992 through March 31, 1992

UNIVERSITY OF NEW MEXICO

CENTER FOR HIGH TECHNOLOGY MATERIALS

Vertical Cavity Surface-Emitting Lasers

For all-optical switching, it is desirable to achieve a bistable optical device that can be optically turned on and turned off while providing optical memory. A photo-transistor/surface-emitting laser (HPT/VCSEL) switch can be optically switched on and off but has no memory, while a photothyristor (PNPN)/VCSEL switch has memory but cannot be optically erased. We have succeeded in achieving a switch with the desired bistable optical characteristics by a simple modification of the PNPN/VCSEL switch. By using a shallow, low dosage proton implantation into the photothyristor, the positive feedback characteristics of the latter can be sufficiently reduced to allow electrically bistable operation in the regime below the holding current level. With the modified photothyristor in series with a VCSEL load, bistable optical characteristics are also obtained. The switching threshold is adjustable optical holding power level in the 10 μW range can be achieved. The optical gain is comparable to that of a HPT/VCSEL switch. Since the bistable switch is structurally almost identical to that of a PNPN/VCSEL switch, the latching and bistable optical switches can both be integrated on the same substrate. Indeed, by simply etching away the upper p-doped layers of the photothyristor structure, a non-latching HPT/VCSEL switch is also obtained. Thus all three switch archetypes are realizable on a common substrate using a single generic epilayer structure.

A theoretical model, which includes both optical and electrical feedback, has been set up to model the bistable switching characteristics. The qualitative features of the bistability and the factors for optimizing such a device can be numerically simulated.

A new technology for implementing a high quality, individually-addressable, surface-mounted VCSEL array is under investigation. This is part of the effort to generate a high-speed, two-dimensional data source for cascadable parallel processing applications. Most of the array results reported thus far have been of the InGaAs strained-layer VCSEL moiety, which cannot be cascaded with sequential switching or logic arrays. (Cheng)

Design of Efficient Green and Blue Surface Normal Second Harmonic Generation Waveguides in $Al_xGa_{1-x}As$

We describe experimental results on single layer ridge and planar waveguides showing reduced diffraction losses from quasi-two dimensional waveguides (Figure 1). We continued our theoretical investigations by examining the design of resonant periodic waveguides. These consist of alternating $\lambda(2\omega)/2$ layers of materials with high and low

$\chi^{(2)}$, which we refer to as the "generating" and "spacing" layers respectively. Periodic resonant enhancement of the SH field elements is achieved by the spacing layers. We model such structures using the properties of the $Al_xGa_{1-x}As$ system. The obvious loss mechanisms are the absorption of the SH signal at green and blue wavelengths by semiconductor materials and the reflection between layers. Absorption makes operation in the blue impossible unless relatively high Al mole fractions are used. However, given high Al compositions, the most important source of loss for blue emitting structures arise from frustrated periodic resonance since the nonlinear susceptibility of the spacing material is not zero. We designed $Al_{.7}Ga_{.3}As/Al_{.9}Ga_{.1}As$ waveguides for 532 nm and 475 nm. These structures are currently being grown by MOCVD and experimental results will be described in a future report. (Malloy)

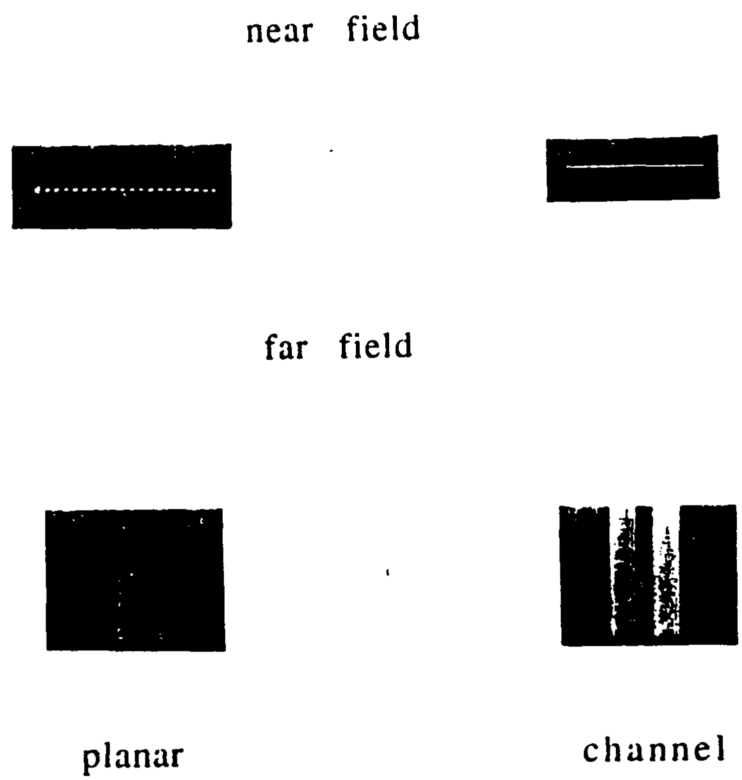

Figure 1. Output Shapes from Waveguides

High-Power Vertical-Cavity Surface-Emitting Semiconductor Lasers

GaAlAs/GaAs and InGaAs/GaAs RPG-VCSEL wafers have been optically pumped above threshold using CW and pulsed Ti:sapphire lasers at wavelengths of 740-950 nm. Two especially interesting results have been obtained:

1. the threshold power has been observed to scale with the lasing area for pumped spot diameters from 10 μm to 1 mm, to within 20% error due to sample non-uniformity. The maximum spot size of 1 mm was dictated by available pump power. These data

were obtained using a 100 fs pulse train from a mode-locked Ti:sapphire laser. The result indicates that ASE is not a major factor in these RPG-VCSEL devices, confirming a result suggested by earlier lasing 1 cm spots pumped by a single-shot dye laser.

2. the threshold and efficiency of the laser is at least as efficient when pumping is directed into a microcavity mode of the RPG-VCSEL resonator than when the spacers are pumped at shorter wavelengths of 750 nm or so. This is significant for diode laser pumping of high-power and compact VCSELs for free-space communication and energy transfer. (McInerney)

Thermal Resistance of Top-Surface-Emitting Vertical-Cavity Diode Lasers

Rigorous analysis of thermal properties of VCSELs requires rather involved numerical calculations. For practical design purposes, it would be very useful to have a simple, albeit approximate, formula for thermal resistance that could easily be used to predict thermal behavior of these devices. We have developed such a formula suitable for top-surface-emitting diode lasers. The formula can be applied to individual emitters and to large-size two-dimensional arrays.

During the next quarter, we plan to apply the thermal resistance formula to calculate temperature distributions in top-surface-emitting VCSELs. (Osinski)

Visualization of Fields in Circuits

We are using electric field induced second harmonic generation (SHG) in thin films of 28/0/100 PLZT to visualize electric fields. The key question that we are trying to answer is how fast does the PLZT react to the application of the electrical field. To answer that question, we constructed fast photoconductive transmission line switches. SHG is probed locally with ps IR pulses (1.06 μm), as the E-field propagates along the transmission line.

The major problem in the previous quarter has been securing *intimate contact* between the probing PLZT film and the circuits. We decided to address that particular problem after having established the technology with PLZT films deposited directly on the circuits, using a sol gel technique. Photoconductive switches were prepared by depositing coplanar striplines directly on semiconductor substrates, such as Si on sapphire and GaAs. The spacing between electrodes is 20 μm. The width of the central electrode is 33 μm. The central electrode and one of the conductive surfaces are at high potential (up to 80 V). The other conductive plane is grounded.

We have studied the switching properties of the circuit. The amplitude of the photoconductive pulse is a linear function of applied voltage, with a slope proportional to the pulse energy. We first studied dc field induced SHG of 1.06-μm ps pulses. The initial dc voltage for visible SHG is observed to be a nonlinear function. Highest dc fields compatible with breakdown are desirable. Therefore, pulsed applied voltages, which have to be synchronized to the optical signal, are now being used.

The sol gel deposition on the circuit is a marked improvement on the "contact" technique used previously. It would, however, be preferable to use sputtered films of PLZT. We are presently depositing circuits directly on the PLZT.

A ps pulse at 530 nm is used to locally short the area between the high and ground electrode. As the wave propagates along the transmission line, a field appears between the central electrode and the electrode originally on high potential. A glass plate with a PLZT thin film is pressed on top of the circuit. The propagating E-field is probed by observing the second harmonic generated by a delayed probe IR picosecond pulse. The two beams (switching beam at 530 nm and probe beam at 1060 nm) are sent through a microscope on the sample. The field induced SHG green light can be observed directly with the eyes. The problem of uniform contact between the PLZT film and the circuit has not been resolved satisfactorily. We are presently experimenting with films of different thickness, and substrates of varying optical quality. Attempts to deposit PLZT directly on the circuit are also being made. (Diels)

PLZT Thin Films

Waveguiding Experiments

Integrated ITO/PLZT/SiO_2/Si and ITO/PLZT/SiO_2/GaAs waveguiding structures are studied. In these structures the SiO_2 layer acts as a buffer layer between the semiconducting substrates and PLZT and facilitates the support of TE and TM waveguide modes. Light is end-fire coupled into this waveguide using a GOX microscope objective. The various TE and TM modes are coupled out using a prism. The angular position of the modes provides a measure of the waveguide effective index. An electric field applied transversely to the direction of propagation using the transparent ITO electrode induces a charge in the effective indices, which in turn causes an angular variation in these out-coupled modes. We have demonstrated an angular shift as large as 0.5° with a calculated field strength of 300 V/mm. The angular shifts are quadratic in the applied field. The observed modulation can be explained in terms of a change in the effective index due to electrooptic effects in the PLZT film and/or possibly electrostrictive effects in the film layers.

Electrooptic Effects in PLZT Thin Films

Field-induced birefringence measurements of PLZT thin film material of composition 28/0/100 show that while the birefringence shift shows a quadratic field-dependence at low fields, saturation behavior occurs for larger external fields. To interpret these electrooptic properties, a phenomenological model, which is based on a generalization of the anharmonic oscillator model, has been formulized. In conjunction with this model, a diagonalization of the Hamiltonian of an oxygen octahedra in a PLZT perovskite structure results in a two-parameter formula, which proves more satisfactory than the nonlinear optical susceptibility expansion approach in describing the electrooptic property of PLZT material.

Surface Normal SHG in PLZT Thin Film Waveguide

The potential use of a PLZT thin film waveguide for surface normal second harmonic generation has been investigated theoretically. The necessary conditions for surface normal second harmonic generation are described. Although current technology of PLZT thin film deposition results in highly oriented polycrystalline film with either [100] or [001] orientation normal to the film, from theoretical analysis, the polycrystalline nature of the film poses no disadvantages for the surface normal second harmonic generation beyond the increase in scattering losses from grain boundaries.

PLZT Thin Film Etching Using Plasma Techniques

The feasibility of patterning PLZT thin films by chemical plasma etching techniques is investigated using HCl and CF_4 in a dc hollow cathode discharge system. The thin films used in the study were deposited on Si substrates using either rf magnetron sputtering or solution deposition methods. Etch rates and variations in film stoichiometry were measured as a function of substrate temperature and etching gas composition. Results show that films are etched in either HCl or CF_4, but substage temperatures above 200°C are required before measurable etch rates occur. The film stoichiometry varies as the etching system parameters are changed, causing considerable variations with substrate and process gas mixture. Etch rates for the solution-deposited films in a CF_4 plasma were an order of magnitude larger than for the sputter-deposited films. The highest etch films (6500 Å /hour) was obtained using a combination of HCl and CF_4, resulting in an etch rate six times greater than those measured using either gas alone. With either of these gases or gas mixtures, complete removal of all material from the substrate can be accomplished. (Wu)

Thermal Properties of Proton-Implanted Top-Surface-Emitting Lasers (PITSELs)

Thermal effects in PITSELs with active region defined by ring contact and proton implantation have been analyzed for the first time. Our self-consistent thermal analysis features realistic distribution of heat sources combined with two-dimensional heat-flux spreading. The results indicate high thermal resistance and intense heating of "junction up" devices.

Electrical Properties of PITSELs

Electrical spreading resistance in PITSELs has been analyzed. Three contact configurations have been considered: annular, circular, and broad-area. Calculations performed for proton-implanted surface-emitting lasers demonstrate that low values of series resistance can be achieved using the broad-area contact configuration.

Thermal Properties of Etched-Well Vertical-Cavity Surface-Emitting Lasers and Two-Dimensional Arrays

We have determined an optimal active-region diameter (16 μm), such that the excess of supplied power over the cw lasing threshold power at the corresponding active-region temperature is maximum. We have shown that the thermal resistance of etched-well VCSELs depends on the pumping conditions. We have also investigated the role of other design parameters, such as thicknesses and doping levels of both cladding layers. Thermal resistance of an optimized structure is as low as 188 K/W, compared to over 400 K/W corresponding to devices reported previously.

We have also modified the single-emitter analysis to study very-large-size two-dimensional VCSEL arrays. The results indicate severe crosstalk for closely packed arrays. We have identified conditions for an array configuration that would not suffer from the excessive cross-talk penalty.

STANFORD UNIVERSITY

Visible Light Sources

Since the last report, we have improved the quality of <100> oriented CdTe grown on <100> GaAs substrates. The orientation is preserved by means of a very thin ZnTe layer at the CdTe/GaAs interface. It has been reported in the literature that growth of a thin ZnTe layer, with thickness on the order of a monolayer, yields a superior quality CdTe overlayer difficult to achieve. We have found that a marked improvement in <100> CdTe surface morphology and process reproducibility can be achieved by using a ZnTe interlayer growth sequence, which is similar to atomic layer epitaxy, i.e., the Te and Zn precursors are alternately introduced into the growth chamber.

The successful procedure is as follows: the GaAs wafer is cleaned using wet chemicals and an *in-situ* prebake for five minutes at 600°C to desorb native oxide. Next, di-isopropyl telluride is passed over the sample for 40 seconds at 330°C at a partial pressure of 4×10^{-4} atm. The chamber is purged for 10 seconds in H_2, and then diethyl zinc is entered into the chamber at 330°C at 1.7×10^{-4} atm. The chamber is purged again for 10 seconds, and then the MOCVD growth of CdTe is begun. (Gibbons/Fejer)

On the device side, we demonstrated CW, 300K operation of an external cavity surface-emitting laser at 850 nm, optically pumped. The fabrication of an electrically pumped sample was begun. A new design for a high speed GaAs photodiode was also started. Using 300 fs pulses at 1.06 μm from a Nd:YAG laser followed by a two-stage fiber-grating compressor, we were able to achieve a >400 GHz electrooptic sampling system. This system will be used to measure the new photodiodes. (Bloom)

We recently designed and fabricated a visible wavelength Fabry-Perot modulator using indirect gap AlGaAs/AlAs quantum wells. Generally, the devices fabricated with the conventional GaAs/AlGaAs alloy require very high accuracy in the growth of the cavity, but are insensitive to errors in the quantum wells. Our device, however, required very tight control of the aluminum concentration in the wells in addition to the control of the cavity. Since the modulator's efficiency is a sensitive function of the spacing between the exciton and the F-P mode, such a ternary modulator is considerably more difficult to fabricate. To reduce possible errors, we used an etch-tuning technique to adjust the

Fabry-Perot resonance after the device was grown and processed. The device operated at 610 nm and exhibited a 30% reflectivity modulation. (Harris)

Though the Fabry-Perot cavity strongly effects the modulator's operation, the device is ultimately limited by the maximum absorption changes in the quantum wells. Previously we found that increasing the barrier's height and the confinement improves the electro-absorption characteristics in InGaAs/(Al)GaAs. Conventionally, the maximum aluminum composition used to increase the confinement is 45%, since the AlGaAs material becomes indirect. However, since the scattering to these indirect valleys is slow, we postulated that AlAs barriers should exhibit superior characteristics. We confirmed this experimentally in GaAs/AlGaAs using simple photocurrent measurements. This improvement in the electro-absorption enabled us to fabricate a reflection modulator with the highest reflectivity modulation to date. The device reflectivity went from 95% in the low absorption state down to the system noise value in the absorbing state. (Fejer, Gibbons, Harris, Bloom)

CALIFORNIA INSTITUTE OF TECHNOLOGY

Nanometer-Scale Selective Growth of GaAs and InGaAs by OMVPE and Application to Quantum Size Effect Semiconductor Lasers

The OMVPE reactor for our quantum-structure work with DEGaCl selective epitaxy, located at the NASA Jet Propulsion Laboratory, has been modified extensively to meet the rigorous requirements of quaternary compound InGaAsP growth and to improve the current AlGaAs growth characteristics.

A self-purging high-purity nitrogen glovebox with gas interlock chambers has been installed to prevent any contamination of growth chamber with oxygen or water vapors. The low-pressure growth capability has been dramatically improved by the complete redesign of the pumping system, including new larger diameter stainless steel tubings, relocation of the pressure transducer, addition of LN cold trap and filters for particulates, complete rebuilding of the pump, and extensive leak testing. Other aspects of the current reactor design have been reviewed for more possible modifications.

More thin film (300Å and 1000Å) deposition processes for silicon nitride, the masking material used in selective growth, have been calibrated and optimized. Silicon nitride layers have been grown on bulk GaAs and OMVPE growth substrates by plasma enhanced chemical vapor deposition. (Vahala)

Ultra-low Threshold Semiconductor Lasers

<u>Passive mode-locking of semiconductor lasers</u>

Passive mode locking of two-section multiple quantum well lasers coupled to an external cavity has been demonstrated before to generate picosecond pulses [1,2]. We have demonstrated wavelength tuning of passively mode-locked lasers by replacing the external cavity mirror by a grating [3,4]. One of the laser sections is biased to act as a saturable absorber. By adjusting the current in the gain section and by rotating the grating, mode-locked operation at the first harmonic of the cavity round-trip frequency is achieved at different wavelengths.

A maximum tuning range of 26 nm was achieved for a laser mode-locked at 561 MHz with minimum mode locking threshold gain currents of 50 mA and grounded absorber section. This broad tuning range is the highest reported ever for passively mode-locked semiconductor lasers. Intensity autocorrelations and pulse widths were measured just above threshold. Measured full width half maxima (FWHM) of the intensity autocorrelations were typically 4.5 ps, with a minimum of 3.5 ps. The pulses are not transform limited and have a typical time-bandwidth product of 2.5, which is about 8 times the transform limit for a hyperbolic secant pulse. Pulse compression may therefore be possible, assuming a linear chirp. At some wavelengths weak satellite pulses were observed at a time delay of 13 ps, corresponding to the round-trip time between the semiconductor facets. These satellite pulses are attributed to a reflection from the AR coated facet (<5%), but may be partially suppressed by the presence of the monolithically integrated saturable absorber.

We are presently investigating the possibility of compressing these pulses to subpicosecond pulse widths using an external grating compressor. (Yariv)

References

[1] S. Sanders, A. Yariv, J. Paslaski, J.E. Ungar, and H.A. Zarem, *Appl. Phys. Lett.*, **58**, 681 (1991)

[2] S. Sanders, T. Schrans, A. Yariv, J. Paslaski, J.E. Ungar, and H.A. Zarem, *Appl. Phys. Lett.*, 59, 1275 (1991)

[3] T. Schrans, S. Sanders, and A. Yariv, *IEEE Photon. Technol. Lett.*, **4**, 323 (1992)

[4] T. Schrans, R. A. Salvatore, S. Sanders, and A. Yariv, in <u>Conference on Lasers and Electro-Optics 1992</u>, 12, OSA Technical Digest Series, paper JThB5, 410 (1992)

PUBLICATIONS

M. Mahbobzadeh, E. Gandjbakhch, E. A. Armour, K. Zheng, S.-Z. Sun, C. F. Schaus, and M. Osinski, *Distributed-feedback vertical-cavity surface-emitting laser with resonant-periodic-gain active region*, Laser Diode Technology & Applications IV, SPIE Laser & Sensor Engineering Symp, OE/LASE'92, Los Angeles, CA, Jan. 19-24, 1992.

M. Mahbobzadeh, E. Gandjbakhch, E. A. Armour, K. Zheng, S.-Z. Sun, C. F. Schaus, and M. Osinski, *Distributed-feedback vertical-cavity surface-emitting laser with resonant-periodic-gain active region*, Laser Diode Technology & Applications IV, SPIE Laser & Sensor Engineering Symp, OE/LASE'92, Los Angeles, CA, Jan. 19-24, 1992.

M. Mahbobzadeh and M. Osinski, *High-power-density pulsed operation of distributed-feedback vertical-cavity surface-emitting laser with resonant-periodic-gain active region,* QELS '92 Conf. on Quantum Electronics & Laser Science, Anaheim, CA, May 10-15, 1992.

W. Nakwaski and M. Osinski, *Thermal resistance of top-surface-emitting vertical-cavity semiconductor lasers and monolithic two-dimensional arrays,* Electron. Lett. (submitted).

W. Nakwaski and M. Osinski, *Thermal properties of proton-implanted top-surface-emitting microlasers in linear and nonlinear regimes,*" LEOS Summer Topical Meeting on Smart Pixels, Santa Barbara, CA, Aug. 10-12, 1992. (submitted).

W. Nakwaski and M. Osinski, *Self-consistent calculation of temperature profiles in proton-implanted top-surface-emitting diode lasers,* Sources and Detectors for Fiber Communications, SPIE International Symp. OE/FIBERS'92, Boston, MA, Sept. 8-11, 1992. (submitted).

W. Nakwaski and M. Osinski, *Thermal analysis of top surface-emitting proton implanted microlasers,* QELS '92 Conf. on Quantum Electronics & Laser Science, Anaheim, CA, May 10-15, 1992.

W. Nakwaski and M. Osinski, *Thermal analysis of top surface-emitting proton implanted microlasers,* QELS '92 Conf. on Quantum Electronics & Laser Science, Anaheim, CA, May 10-15, 1992.

W. Nakwaski, M. Osinski, M. Bugajski, and B. Mroziewicz, *Self-consistent semi-analytical approach to thermal and electrical characteristics of etched-well surface-emitting diode lasers,* IQEC'92 XVIII Int. Quantum Electronics Conf., Vienna, Austria, June 14-19, 1992

M. Osinski, *Control of thermal problems in monolithically integrated vertical-cavity surface-emitting semiconductor laser arrays,* 2nd IEEE International Workshop on Photonic Networks, Components and Applications, Montebello, Quebec, Canada, March 9-11, 1992. (invited paper)

M. Osinski and W. Nakwaski, *Thermal properties of etched-well surface-emitting diode lasers and two-dimensional arrays,* Laser Diode Technology & Applications IV, SPIE Laser & Sensor Engineering Symp., OE/LASE'92, Los Angeles, CA, Jan. 19-24, 1992.

P. Zhou, J. Cheng, C.R. Schaus, S.-Z. Sun, C. Hains, K. Zheng, E. Armour, W. Hsin, D.R. Myers, and G.A. Vawter, *Cascadable, Latching Photonic Switch with high Optical Gain by the Monolithic Integration of a Vertical-Cavity Surface-Emitting Laser and a PNPN Photothyristor*, IEEE Phot. Tech. Lett., 3, 1009-1012 (November 1991)

P. Zhou, J. Cheng, C.F. Schaus, S.-Z. Sun, C. Hains, K. Zheng, A. Torres, D.R. Myers, and G.A. Vawter, *High-Performance, Latchable Optical Switch and Logic Gates Based on the Integration of Surface-Emitting Lasers and PNPN Photothyristors*, Appl. Phys. Lett. 59, No 20, 2504-2506 (November 11, 1991)

P. Zhou, J. Cheng, C.F. Schaus, S.-Z. Sun, D.R. Myers, and G.A. Vawter, *Surface-Emitting Laser-Based Bistable Optical Switching Device*, Appl. Phys. Lett. 59, No. 21, 2648-2650 (Nov. 18, 1991)

P. Zhou, J. Cheng, C.F. Schaus, S.-Z. Sun, D.R. Myers, and G.A. Vawter, Versatile *Bistable Optical Switches and Latching Optical Logic Gates Using Integrated Photothyristors and Surface-Emitting Lasers*, 1991 International Electron Device Meeting Technical Digest, 611-614 (Dec. 1991)